

# Kent Academic Repository

## Full text document (pdf)

### Citation for published version

Volcke, C. and Gandhiraman, R.P. and Gubala, V. and Raj, J. and Cummins, Th. and Fonder, G. and Nooney, R.I. and Mekhalif, Z. and Herzog, G. and Daniels, S. and Arrigan, D.W.M. and Cafolla, A.A. and Williams, D.E. (2010) Reactive amine surfaces for biosensor applications, prepared by plasma-enhanced chemical vapour modification of polyolefin materials. Biosensors

### DOI

<https://doi.org/10.1016/j.bios.2009.12.034>

### Link to record in KAR

<http://kar.kent.ac.uk/45241/>

### Document Version

Author's Accepted Manuscript

#### Copyright & reuse

Content in the Kent Academic Repository is made available for research purposes. Unless otherwise stated all content is protected by copyright and in the absence of an open licence (eg Creative Commons), permissions for further reuse of content should be sought from the publisher, author or other copyright holder.

#### Versions of research

The version in the Kent Academic Repository may differ from the final published version.

Users are advised to check <http://kar.kent.ac.uk> for the status of the paper. **Users should always cite the published version of record.**

#### Enquiries

For any further enquiries regarding the licence status of this document, please contact:

[researchsupport@kent.ac.uk](mailto:researchsupport@kent.ac.uk)

If you believe this document infringes copyright then please contact the KAR admin team with the take-down information provided at <http://kar.kent.ac.uk/contact.html>

**Reactive amine surfaces for biosensor applications, prepared by  
plasma-enhanced chemical vapour modification of polyolefin  
materials**

C. Volcke<sup>1,2,\*,\$</sup>, R.P. Gandhiraman<sup>1,\*</sup>, V. Gubala<sup>1</sup>, J. Raj<sup>3</sup>, Th. Cummins<sup>1,4</sup>, G.  
Fonder<sup>5</sup>, R. Nooney<sup>1</sup>, Z. Mekhalif<sup>5</sup>, G. Herzog<sup>3</sup>, S. Daniels<sup>1,6</sup>, D.W.M. Arrigan<sup>3</sup>, A.A.  
Cafolla<sup>1,4</sup> and D.E. Williams<sup>1,7</sup>

<sup>1</sup> *Biomedical Diagnostics Institute, Dublin City University, Glasnevin, Dublin 9, Ireland.*

<sup>2</sup> *Research Centre in Physics of Matter and Radiation (PMR), University of Namur (FUNDP), 61 rue de Bruxelles, B-5000 Namur, Belgium.*

<sup>3</sup> *Biomedical Diagnostics Institute Programme, Tyndall National Institute, University College Cork, Cork, Ireland.*

<sup>4</sup> *School of Physical Sciences, Dublin City University, Glasnevin, Dublin 9, Ireland.*

<sup>5</sup> *Laboratory of Chemistry and Electrochemistry of Surfaces, University of Namur (FUNDP), 61 rue de Bruxelles, B-5000 Namur, Belgium.*

<sup>6</sup> *National Center for Plasma Science and Technology, Dublin City University, Glasnevin, Dublin 9, Ireland.*

<sup>7</sup> *MacDiarmid Institute for Advanced Materials and Nanotechnology, Department of Chemistry, University of Auckland, Private Bag 92019, Auckland 1142, New Zealand.*

## **Abstract**

Functionalization of the plastic chips for selective immobilization of biomolecules is one of the key challenges to be addressed in commercialization of the next-generation point-of-care (POC) diagnostics devices. Multistep liquid-phase deposition process requires a large quantity of solvent to be used in anhydrous conditions, providing quantity of industrial liquid waste. We, in this work, have demonstrated a solventless plasma-based process that integrates low-cost, high throughput, high reproducibility and ecofriendly process for the functionalization of POC device platforms. Amine functionalities have been deposited by plasma-enhanced chemical vapour deposition

(PECVD) using a new precursor. For a successful and efficient plasma functionalization process, an understanding of the influence of plasma process parameters on the surface characteristics is essential. The influence of the plasma RF power and the deposition time on the deposited amount of amino functionalities and on their capacity to immobilize nano-objects (i.e., nanoparticles) and biomolecules (i.e. DNA) was examined. Surface properties were related to the binding capacity of the films and to the amino content, as revealed by the “nanoparticle approach” and DNA attachment experiments. The key process determinants were to have a sufficient power in the plasma to activate and partially fragment the monomer but not too much as to lose the reactive amine functionality, and sufficient deposition time to develop a reactive layer but not to consume or erode the amine reactivity. An immunoassay performed using human immunoglobulin (IgG) as a model analyte shows an improvement of the detection limit by two orders of magnitude beyond that obtained using devices activated by liquid-phase reaction.

Keywords: biosensors, polymer, plasma enhanced chemical vapour deposition, nanoparticle, DNA, immunoassay.

\* Those authors contributed equally

§ To whom correspondance should be addressed. Phone: +32 81 72 54 30. Fax: +32 81 72 47 18. E-mail : [cedric.volcke@fundp.ac.be](mailto:cedric.volcke@fundp.ac.be)

## 1. Introduction

Immobilization of biomolecules onto surfaces, and particularly onto polymeric substrates, is a key issue for the fabrication of next-generation biosensors and biomedical diagnostic devices. Zeonor<sup>®</sup>, a type of cycloolefin polymer (COP), is one such polymer presenting excellent optical properties, good chemical resistance, ease of fabrication and cost effectiveness (Diaz-Quijada 2007, Kameoka 2001). Though several biomolecule immobilization techniques have been intensively reported in the literature during the last decade, only a few recent communications address the issue of activation of cycloolefin polymers (Jönsson 2008, Laib and McCraith 2007, Raj 2009).

In general, biomolecular immobilization is classified as chemical (Kwon 2006, Mateo-Marti 2005) or physical (LaGraff and Chu-LaGraff 2006, Sethuraman 2004) immobilization. Chemical immobilization, through covalent linkage of biomolecules onto surfaces has shown good reproducibility and coverage (compared to physical adsorption) and therefore has become predominant in the research literature. In such cases, liquid-phase deposition of functional groups, further attaching proteins or nucleic acids, on activated surfaces is a routinely used procedure. For example, one of the most studied methods is the self-assembly of aminosilanes on oxidized silicon surfaces (Choi 2006, Oh 2002, Song 2008, Zhang and Srinivasan 2004). These modification procedures have still not been extensively investigated for polymers, for which physical immobilization is the dominant methodology.

Liquid-phase deposition chemistry for attachment of aminosilanes onto surfaces, as broadly studied, is demanding (water-free environment, time-consuming, hazardous materials) and hardly applicable to large industrial production requirements (Kurth and Bein 1995). Gas-phase deposition of amine reactive groups, using plasma

enhanced chemical vapour deposition (PECVD) for example, overcomes the drawbacks of liquid-phase deposition (Foose 2007, White and Tripp 2000). PECVD, a versatile surface engineering technique, has proven to be an excellent tool for surface modification at low temperatures (Dudek 2009a, Favia 2001, Gandhiraman 2007, Muguruma and Kase 2006). In principle, it offers significant advantages: uniformly diverse functional coating deposition on various surfaces (even on complex 3D structures); precise control of thickness; and adaptability for large mass production processing. Surface amination by PECVD has previously been studied using, e.g., ethylene diamine (EDA) as precursor on different substrates (Gomathi 2008, Jung 2006, Slocik 2006). Unfortunately, the adhesion and stability of these PECVD deposited EDA films onto cycloolefin polymers were very poor (unpublished data). The results were interpreted to imply merely physisorption and not reactive chemisorption of EDA molecules onto the polymeric surface.

Therefore new precursors, potentially presenting good adhesion and stability on polymeric surfaces, and also offering amine groups for subsequent reaction, are needed. In this context, 3-(aminopropyl) triethoxysilane (APTES), commonly used for liquid-phase deposition of amine functional groups (Moon 1997, Qian 1999, Gu and Cheng 2008, Simon 2002, Sridharan 2008) is expected to present all the requirements needed. Previous investigations of chemical vapour deposition (CVD) on silicon substrate at elevated temperatures highlighted its suitability (Arroyo-Hernandez 2006). However, to be appropriate for polymeric surfaces, PECVD deposition has to be used. PECVD deposition of APTES is expected to result in reproducible silanized surfaces containing reactive amine groups, with good adhesion to cycloolefin polymer through a siloxane network. The characteristics of PECVD coatings are highly

dependent on the nature of the substrate, the precursor and the plasma characteristics including input power and deposition time (Di Mundo 2007).

In this paper, we present a detailed investigation on the optimization of the reactive-amine content of a deposited amino-film on a COP surface, for improved biomolecule attachment by appropriate choice of experimental parameters. Plasma conditions, for example, the plasma electron density, were shown to have significant effects on the performance of the coating. Aminated coatings have been prepared by PECVD of APTES onto a Zeonor<sup>®</sup> substrate. The influence of the plasma RF power and the deposition time on the deposited amount of amino functionalities and on their capacity for immobilizing nano-size objects (nanoparticles) and biomolecules (ssDNA) was investigated. Water contact angles, atomic force microscopy (AFM), ellipsometry and polarization modulation infrared reflection-absorption spectroscopy (PMIRRAS) have been used for physical and chemical characterization. Fluorescence microscopy has been performed to quantify the binding of an amine-reactive fluorophore and a labelled ssDNA. Reactive amine coverage on the surface has been evaluated by attachment of nanoparticles, visualised by atomic force microscope (AFM). This was a particularly effective and simple evaluation tool. An immunoassay was performed using human immunoglobulin G (IgG) as a model analyte and the detection limit was compared to that of the liquid-phase deposition process. We describe overall a procedure for determining the optimal deposition condition to create a surface presenting a high amount of amino groups, capable of attaching the highest amount of biomolecules.

## **2. Experimental Part**

### **2.1. Materials**

Plain Zeonor<sup>®</sup> slides (Zeonor 1060R, Zeon, Japan) were obtained from Åmic AB (Uppsala, Sweden). 3-aminopropyltriethoxysilane (APTES), Lissamine<sup>®</sup> rhodamine B sulfonyl chloride ( $\lambda_{exc.} = 532$  nm excitation and  $\lambda_{em} = 550$  nm emission) and acetonitrile were purchased from Sigma Aldrich and used without further treatment.

### **2.2. PECVD system**

The plasma deposition was carried out using a computer controlled Europlasma CD 300 PECVD system. The aluminum vacuum chamber was connected to a Dressler's CESAR 136 RF power source operating at 13.56 MHz, capable of generating a maximum of 600 W RF power, supplied with an automated impedance match-box for effective RF energy input to the plasma. In the PECVD process, the input radio frequency (RF) current/ voltage was supplied to the powered electrode, a 24 cm x 21 cm plate with a 6 cm diameter hole in the middle, placed slightly below the top of the chamber. The powered electrode was cooled with running water. A 24 cm x 21 cm x 1.2 cm electrically isolated (floating potential), water cooled hollow metallic setup placed 10 cm below the powered electrode was used as a substrate holder. The detailed description and a schematic of the system used is shown elsewhere (Dudek 2009b, Gandhiraman 2009).

### **2.3. Surface preparation**

Zeonor<sup>®</sup> slides were first cleaned with dry air before being loaded in the plasma chamber. The system pressure was pumped down to a base pressure of 25 mTorr. APTES precursor was stored in a container (connected to the vacuum chamber). As

the vapour pressure of APTES is less than 10 Torr at 100° C, the APTES container and the supply line from source to chamber was heated at 80° C. Plasma pre-treatment for cleaning and activation was carried out using a mix of argon (50 sccm) and oxygen (50 sccm) plasma at 250 watt RF power for 3 minutes. The oxygen supply was then closed and the plasma RF power was decreased to the desired value (7 watt, 14 watt or 25 watt). APTES was then introduced in the chamber for the required deposition time (2 min, 4 min or 8 min). The operating pressure was ~ 70 mTorr.

## ***2.4. Surface characterization***

### *2.4.1. Ellipsometry*

The thickness of the APTES coating on Zeonor<sup>®</sup> was characterized using J.A. Woollam Co., Inc EC-400, M-2000UI Spectroscopic Ellipsometer. All layers were modelled as a simple silicon dioxide dispersion layer to extract an effective thickness.

### *2.4.2. Plasma electron density measurement: Hairpin probe*

The hair pin probe is a diagnostic technique for measuring absolute electron density in the discharge using a microwave resonance probe (Dudek 2009b). The principle of the probe is based on measuring the dielectric constant of the plasma surrounding the resonant structure. The probe, consisting of two parallel wires, short circuited at one end and open at the other, resembles a hairpin. The typical length of the hairpin was 1-2 cm. The microwave resonance of the hairpin was used to determine electron density.

### *2.4.3. Water contact angles*

The film wettability was analyzed by measuring the water contact angle of the film surface (First Ten Angstroms FTA200 contact angle analyser). High purity HPLC grade water (Sigma Aldrich) was used for the measurement.

#### 2.4.4. Roughness measurements - Atomic force microscopy (AFM)

AFM examinations were performed in ambient air with a commercial microscope (Dimension 3100 controlled by a Nanoscope IIIa controller, Digital Instruments, Santa-Barbara – CA, USA), in the Tapping-Mode™, using standard silicon cantilevers (BudgetSensors® , Innovative Solutions Bulgaria Ltd, Bulgaria) with a 7 nm radius of curvature and a 42 N.m<sup>-1</sup> spring constant (nominal values). Topographic images were recorded at a scanning rate of 1-2 Hz, and a resonance frequency of about 300 kHz (nominal value). The background slope was resolved using a first order polynomial function. No further filtering was performed. The surface roughness of substrates and PECVD deposited APTES coatings was evaluated over 3 images (5 µm x 5 µm) and the standard deviation was then calculated. The root-mean-square roughness (Rrms) was defined as the average of height deviations taken from the mean plane (Haidopoulos 2007).

#### 2.4.5. Polarization modulation infrared reflection absorption spectroscopy (PMIRRAS)

Appropriate substrates had to be prepared for infrared reflection-absorption spectroscopy since surfaces highly reflecting to IR light are required for this technique. The substrates were obtained by sputtering gold on cleaned silicon wafer (with piranha solution, followed by extensive rinsing). Zeonor® was dissolved in xylene (0.25 gr/l) by 10 min sonication and the solution was filtered through a

millipore 0.2  $\mu\text{m}$  filter. The solution was finally spin coated onto the gold coated silicon substrates (Jönsson 2008). PMIRRAS spectra of the COP-coated gold surfaces, before and after APTES deposition were recorded on a Bruker Equinox 55-PMA37 spectra equipped with liquid nitrogen cooled mercury cadmium-telluride (MCT) detector and a zinc-selenide photoelastic modulator. The infrared light was modulated between s- and p-polarization at a frequency of 50 kHz. The incident angle upon the sample surface was around  $85^\circ$ . Signals generated from each polarization ( $R_s$  and  $R_p$ ) were detected simultaneously by a lock-in amplifier and used to calculate the differential surface reflectivity  $(\Delta R/R) = (R_p - R_s)/(R_p + R_s)$ . The spectra were an average of 640 scans and were taken at a spectral resolution of  $2\text{ cm}^{-1}$ .

#### 2.4.6. Nanoparticle (NP) approach

##### *Preparation of silica NPs*

Silica NP's were prepared using a microemulsion method (Arriagada and Osseo-Asare 1999). The microemulsion was formed by adding water (0.96 ml) to a mixture of cyclohexane (15 ml), *n*-hexanol (3.6 ml) and Triton<sup>®</sup> X-100 (3.788 g). Following this, tetraethylorthosilicate (TEOS) (0.2 ml) and  $\text{NH}_4\text{OH}$  (0.16 ml) were added to start the growth of the silica NPs. The reaction was stirred for 24 hrs, after which TEOS (0.1 ml) was added with rapid stirring. After 30 minutes 3-trihydroxysilylpropylmethylphosphonate sodium salt (THPMP) (0.08 ml) was added with stirring to prevent aggregation of the nanoparticles. After a further 5 minutes 3-aminopropyltrimethoxysilane (APTMS) (0.02 ml) was added for conjugation to the amine functionalized surfaces. The NPs were separated from the solution with the addition of excess absolute ethanol and centrifuged twice with ethanol and once with deionized water (Heraeus, Biofuge pico). Sonication was used between the washing

steps to resuspend the NPs. The NPs were dispersed in deionised water, at 2.0 mg/ml and stored in the dark at 4° C.

#### *Conjugation of NPs to amine functionalized surfaces*

The COP slides coated with amine groups were first dipped in an aqueous solution containing glutaraldehyde (2 wt %) for 24 hrs. Following this the slides were dipped in an aqueous solution containing NPs (2.0 mg / ml) for a further 24 hrs. The amount of surface coverage was determined using atomic force microscopy.

#### *AFM imaging and analysis*

AFM imaging was performed in the same conditions as the roughness measurements (Tapping-Mode™, Si cantilevers with nominal value of 7 nm radius of curvature, 42 N.m<sup>-1</sup> spring constant and 300 kHz resonance frequency). Topographic images were recorded at a scanning rate of 1-2 Hz. The background slope was resolved using a first order polynomial function. No further filtering was performed. Nanoparticle counting was performed using the commercial Scanning Probe Image Processor program (SPIP™, version 4.1.8.0 from Image Metrology).

#### 2.4.7. Fluorescence

Attachment of the fluorophores to amino-functionalized Zeonor® substrates was achieved by immersing the samples for 1 hr in a 0.23 mM Lissamine® rhodamine B sulfonyl chloride in acetonitrile. 100 µl triethylamine was added to 100 ml of the lissamine solution. Samples were then rinsed with distilled water and sonicated for 5 minutes in a 0.1 % sodium dodecyl sulfate (SDS) solution. Following, the substrates were rinsed again with distilled water and dried under a nitrogen stream. The fluorescence intensity after lissamine attachment was measured using a plate scanner (GMS 418 scanner: Genetic Microsystems, Affymetrix). For the immobilization of

fluorescently labelled DNA, slides were activated with 1,4-phenyldithioisocyanate (PDITC, ABCR) linker by incubation of amino-coated Zeonor<sup>®</sup> substrate for 3 hrs in a 5 mM solution of PDITC in anhydrous acetonitrile containing 1 wt % of pyridine. The slides were then washed three times in DMF and dried in a stream of nitrogen.

Afterwards,  $50 \times 10^{-7}$  M solution of the polynucleotide (5'-fluorescein labelled, 3'- C6 amino linker) was prepared by diluting the stock solution of ssDNA in 10 mM 2-(N-morpholino)ethanesulfonic acid (MES) buffer (Sigma-Aldrich) containing 5 mM 1-ethyl-3(3-dimethylaminopropyl)carbodiimide (EDC, Pierce), 10 mM MgCl<sub>2</sub> (Sigma-Aldrich) and 0.33 mM N-hydroxysulfosuccinimide (NHSS, Pierce). Microarraying was performed on a microarray spotter (50-60  $\mu$ m spots at 500  $\mu$ m spacing, centre to centre). For post-processing, the slides were sonicated in 1% SDS for 5 minutes to remove the non-covalently bound ssDNA from the surface and then rinsed extensively with deionized water. The fluorescence intensity was then measured by the plate scanner.

### ***2.5. Immunoassay***

APTES modified slides were immersed in a 25 mM PDITC in N,N-dimethylformamide (DMF):pyridine (9:1 v/v) solution for two hours. The slides were then rinsed with DMF and methanol and dried under a stream of nitrogen. For the immunoassay, 1  $\mu$ l of the capture antibody goat anti-human immunoglobulin G ( $\alpha$ IgG) (0.1 mg/ml) solution, at the desired concentration, was loaded on a PDITC-modified slide and incubated at 37° C for one hour. The surfaces were then washed with phosphate buffered saline solution (PBS) with Tween 20 (0.2 % v/v) and then with PBS. The slides were subsequently immersed in a bovine serum albumin (BSA)

(3 % w/v) solution for one hour. After rinsing with PBS, different concentrations of the model analyte IgG (0.02 pg/ml – 0.2 mg/ml) were loaded (1  $\mu$ l) and incubated at 37° C for one hour. The slides were washed with PBS, then the detection antibody Cy-5 labelled g $\alpha$ IgG (1  $\mu$ l of 0.3 mg/ml) was printed using BioRobotics pins (1  $\mu$ l) and incubated at 37° C for 1 hour. The device surfaces were subsequently washed with PBS containing Tween 20 (0.2 %) solution twice, with PBS once and dried under a stream of nitrogen. The immunoassay was then ready for detection by measuring the fluorescence intensity. Fluorescence images were acquired with an Olympus BX51 Epi-fluorescent microscope equipped with an Olympus DP71 Camera and appropriate filters. The excitation was obtained using an X-Cite Lamp Series 120 PC.

### 3. Results and Discussion

PECVD deposited APTES coatings have been prepared under different conditions of RF plasma power (7 watt, 14 watt and 25 watt) at a fixed deposition time (4 min), and of deposition time (2 min, 4 min and 8 min) at a fixed RF plasma power (14 watt). We first present results obtained on coating deposited at fixed deposition time and further at fixed RF plasma power followed by the selection of the one in each batch having the highest amount of amino-groups. The binding capacity was analyzed through the nanoparticle attachment experiment as well as by fluorophore and DNA attachment. Finally immunoassay results are presented.

#### 3.1. At fixed deposition time of 4 minutes

For coatings generated under the three RF plasma power conditions used (7 watt, 14 watt and 25 watt), the layer thickness as measured by ellipsometry, the water contact angle and the surface roughness (as measured by AFM) are presented in **Table 1**.

Although the variations highlighted in **Table 1** are relatively small, the thickness clearly and significantly increased, at first steeply, and then more gradually, with increase of RF plasma power. Plasma electron density measurements using the hair pin probe (see Supporting Information) show that electron density (and hence plasma density) increased with increasing RF plasma power. The increased deposited layer thickness can therefore be explained as a consequence of the enhanced decomposition of the reactants induced by an increase in the plasma density, as previously reported for similar systems (Kulisch 1998, Zajickova 1999). The

equilibrium water contact angle shows that the hydrophilicity of the three surfaces were relatively similar: water contact angle around 55-60°. Thus the coatings had similar hydrophilicity and surface energy, independently of the plasma power used. This water contact angle is similar to that found in the literature for liquid-phase deposited APTES on silicon oxide surfaces (Cho and Ivanisevic 2004). AFM Tapping-Mode™ images of the three PECVD deposited film surfaces (Supporting Information) show that all coatings were very smooth (RMS roughness values between 0.7 and 1.4 nm, **Table 1**). There was therefore a uniform deposition over the polymeric surface, independently of the plasma power condition used. It is noteworthy that roughness modifications due to uncontrolled aminosilane polymerization on the surface, as sometimes observed on liquid-phase deposition of APTES on silicon surfaces, were not present here, illustrating one advantage of the PECVD deposition process.

Polarization modulation infrared reflection-absorption (PMIRRAS) spectra are shown in **Figure 1**. These spectra contain several vibrational features that can be assigned to the deposited aminosilane, the most prominent being located in the 1300-1000 cm<sup>-1</sup>, 1800-1500 cm<sup>-1</sup> and 3500-3200 cm<sup>-1</sup> region (**Figure 1**). These infrared features, associated with silane and amine vibrations, are missing on the COP substrate spectrum.

Bands in the first region have three main components at 1265 cm<sup>-1</sup>, 1220 cm<sup>-1</sup> and 1199 cm<sup>-1</sup> (**Figure 1**). The vibrational peaks at 1265 cm<sup>-1</sup> can be assigned to the symmetric deformation vibration of the CH<sub>3</sub> group attached to silicon atom,  $\delta_s(\text{Si-CH}_3)$  (Wavhal 2006). The peak at 1220 cm<sup>-1</sup> can be assigned to Si-CH<sub>2</sub>-R deformation (Socrates 2004). Finally, the band at 1199 cm<sup>-1</sup> can be assigned to Si-O-C and C-N vibrations (Socrates 2004, Truica-Marasescu and Wertheimer 2008). Some variations

in the IR absorption peak intensities according to plasma power conditions are observed. We can reasonably assume an isotropic orientation of the plasma deposited molecules in the coating and an independency of the orientation of the (fragmented) molecules with the deposition conditions used, so that IR peak intensities can be correlated to the amount of molecules/functional groups in the coating, without taking into account orientation effects. The analysis of the peak intensities/area in the 1300-1000  $\text{cm}^{-1}$  region (**Figure 1**) revealed peaks were generally more intense for the 7 watt coating, with a decreasing tendency in peak intensities/area as the RF plasma power increased. Thus, although the deposited layer thickness increased with increasing power, the silicon content of the layer decreased.

In the second region (**Figure 1**), the presence of carboxylic group vibrational peaks (at 1754  $\text{cm}^{-1}$  and 1734  $\text{cm}^{-1}$  associated to  $\nu(\text{C}=\text{O})$  ester and  $\nu(\text{C}=\text{O})$  carboxylic acid) was observed (Dreesen 2007, Finke 2009, Salmain 2006). The peak intensity/area varied following the trend:

$$I(\text{C}=\text{O})_{25 \text{ watt}} < I(\text{C}=\text{O})_{7 \text{ watt}} < I(\text{C}=\text{O})_{14 \text{ watt}}$$

Oxygenated surface species could originate from the initial surface treatment. However as the pretreatment conditions were identical for all coatings, it should not have affected the C=O peak intensity. Therefore this trend is assumed to arise from dissociation of the silane to produce ethoxy radicals. The variations in the C=O bond content with an increasing RF plasma power is reasoned to be due to reactions of the carboxylic groups with radicals from APTES monomer molecules, as previously obtained under similar conditions using different monomers (Bae 2007). As the radicals created in the plasma differ according to plasma power conditions, they would react differently with the surface and a variable C=O vibration intensity/area is thus expected.

Spectral signatures characteristic of vibrations associated with amine functions can be identified in two regions of the spectra. The broad band located in the 1650-1600  $\text{cm}^{-1}$  range (**Figure 1**) can be assigned to primary  $\text{NH}_2$  group vibrations. With increasing RF plasma power from 7 watt to 25 watt, this amine peak was slightly shifted towards lower wavenumbers, indicative of the transformation of free amine into hydrogen-bonded amine (Kanan 2002). In the 7 watt, 14 watt and 25 watt coating a spectrum, this peak was centred at 1640  $\text{cm}^{-1}$ , 1625  $\text{cm}^{-1}$  and 1595  $\text{cm}^{-1}$ , respectively. A broad band associated with the presence of primary amines was also observed on all coatings in the range 3500-3200  $\text{cm}^{-1}$  (**Figure 1**).

The  $\text{NH}_2$  vibration mode intensity / peak area in the 1650-1600  $\text{cm}^{-1}$  and 3500-3200  $\text{cm}^{-1}$  ranges were highest in the 7 watt coating spectrum. The decrease in the  $\text{NH}_2$  IR absorption bands with increase in the RF plasma power implies a decrease in the amine content of the coatings. The results indicate that, at the lowest power, the silane was activated and could react with the surface, but was not significantly dissociated. With increasing power, the silane became fragmented, with amine functions being lost and the layer being built through reaction of ethoxy radicals.

### **3.2. At fixed power**

At a fixed plasma power (14 watt), as the deposition time was increased, the thickness of the APTES coating also increased (**Table 1**). The values for the water contact angle, presented in **Table 1**, showed that the hydrophilicity did not change. Only small variations in contact angle were observed when compared to the samples deposited at different plasma power (at fixed deposition time).

The analysis of AFM Tapping-mode<sup>TM</sup> images of the three PECVD deposited films (see Supporting Information) showed that all coatings were very smooth (RMS

roughness values between 0.7 and 1.3 nm, **Table 1**). No specific trend can be extracted from the roughness measurements. Values were similar for all conditions, including plasma power variation, indicating the invariance of the roughness for the range of the deposition condition studied.

**Figure 2** highlights changes in the PMIRRAS spectra of PECVD deposited APTES on COP surfaces with varying deposition time, at fixed RF plasma power (14 watt). The peaks in the 1100 -1300 $\text{cm}^{-1}$  region, associated with silane vibration, all increased with increasing deposition time. The peak centred around 1200-1170  $\text{cm}^{-1}$  assigned to Si-O-C rocking and C-N vibrations increased slightly in wave number (1172  $\text{cm}^{-1}$ , 1199  $\text{cm}^{-1}$  and 1194  $\text{cm}^{-1}$  for 2 min, 4 min and 8 min coatings, respectively) with increase in deposition time (Socrates 2004). The peak centred on 1230-1210  $\text{cm}^{-1}$ , assigned to Si-CH<sub>2</sub>-R vibration mode also slightly shifted to higher wavenumber as the deposition time was increased (1210  $\text{cm}^{-1}$ , 1222  $\text{cm}^{-1}$ , 1230  $\text{cm}^{-1}$  for 2 min, 4 min and 8 min, respectively). The peak intensities associated with amine and carboxylate functions, at around 1700  $\text{cm}^{-1}$  and 3200-3500  $\text{cm}^{-1}$  did not increase monotonically with increasing deposition time. Instead, they followed the trend:

$$[\text{NH}_2, \text{C}=\text{O}]_{8 \text{ min}} < [\text{NH}_2, \text{C}=\text{O}]_{2 \text{ min}} < [\text{NH}_2, \text{C}=\text{O}]_{4 \text{ min}}$$

There were also changes in peak position in the amine region (region 2, **Figure 2**). The 2 min coating presented a small peak (area: 0.12) centred at 1594  $\text{cm}^{-1}$ . The 4 min coating had a more intense peak (area: 1.81) centred at 1624  $\text{cm}^{-1}$ . After 8 min deposition, the peak (area: 1.23) was shifted to 1644  $\text{cm}^{-1}$ . Shifts to lower wavenumber indicate an increase in the hydrogen bonding character of the amino group (Kanan 2002).

As deposition time increased, the thickness of the deposited layer increased. However, for deposition times longer than 4 min, the ester and amine amount decreased with

increasing deposition time. We rationalize this by the fact that, during the plasma deposition of films, the growing film surface is exposed to the plasma. Therefore, as the plasma exposure time is increased, the reactive groups on the growing film surface, including amines and esters, might undergo functional changes induced by plasma generated species such as ions and charged radicals (Kim 2003). The maximum peak intensity assigned to amines, measured by PMIRRAS, was observed at deposition time of 4 min. This appeared to be the optimal condition at which a reasonable mass of amines could be formed on the surface. Longer exposure to the plasma seemed to trigger structural changes of the functional groups of interest.

### **3.3. Reactivity and immobilization capabilities of the amino coated COP surfaces.**

The presence of free reactive amines on the COP surface can be confirmed and quantified by studying the coupling reactivity to functionalized nanoparticles. In the nanoparticle approach (see experimental section), a homo-bifunctional cross-linker, glutaraldehyde, was used to attach the amino-functionalized silica nanoparticles (NP) to the amino-coated Zeonor<sup>®</sup> surface. The nanoparticle density/distribution was then imaged using AFM. The expectation was that this would be influenced significantly by the content, orientation, and density of reactive amino groups on the surface. Tapping-mode<sup>TM</sup> AFM images of nanoparticles linked onto the COP substrate can be found in the Supporting Information. **Figure 3** shows the number of nanoparticles attached per micron square on the different APTES coated COP surfaces. As expected, the uncoated Zeonor<sup>®</sup> surface was unreactive. At fixed deposition time (4 min), the NP number bound was very similar for plasma powered at 7 and 14 watt.

Then, it declined with increase of power to 25 watt. At fixed RF power (14 watt), the NP number bound increased to a maximum value with increasing deposition time. So, coatings presenting the highest amount of free  $\text{NH}_2$  (as indicated by PMIRRAS spectroscopy) attached the highest amount of nanoparticles and hence had the highest amine reactivity. In other words, larger amine content resulted in better nanoparticle attachment capacity. Although the nanoparticle distribution cannot directly reveal the amount of amine groups on the surface, it can provide an idea of their density, distribution and their capability to bind nano-objects. However, the fact that the bound NP amount per  $(\mu\text{m})^2$  was similar on two coating does not mean they have the same properties. This nanoparticle approach has some limitations mainly due to surface saturation, which makes the method dependent on nanoparticle size for example.

To further investigate the reactivity of the preselected coatings (14 watt – 4 min and 7 watt – 4 min) and to determine the most appropriate one for biosensor application, the coupling reaction of aminated surfaces to a fluorophore, Lissamine<sup>®</sup> rhodamine B sulfonylchloride, specifically binding to amino groups, was studied. **Figure 4** shows on the 14 watt – 4 min coating double intensity that on the 7 watt – 4 min coating, indicating the presence of twice the amount of reactive surfacial amino groups, if we assume one fluorophore per amino group. These measurements highlight the role of nano-object size on surface attachment. Although both selected coatings presented similar nanoparticle attachment, they behaved significantly differently while attaching fluorophores. This is probably due to size effects: the nanoparticles used were  $\sim 60$  nm in diameter; the fluorophore has a size in the nanometre range. Where every surfacial amine functional group can be identified by a fluorophore, it is not the case with the nanoparticles used. This effect should be taken

into account while elaborating functional surfaces for biosensors application, according to the size of the nano-object to be attached on the surface.

To demonstrate the performance of the surface in capturing biomolecules, DNA attachment was performed. Fluorescence intensities measured after attachment of a polynucleotide, as presented in **Figure 4**, indicated the 14 watt coated surface to be three times more performant in attaching DNA molecules than the 7 watt coated one. However, the PMIRRAS NH<sub>2</sub> peak area was twice larger in the 7 watt deposited films than in the 14 watt film. This indicates that, whilst there could have been more amines in the 7 watt coating than in the 14 watt, either they were not present at the surface or they were not reactive. It seems unlikely that the coating varied significantly in its composition through its thickness. We deduced earlier that one effect of increasing the plasma power was to increase fragmentation of the silane. Thus, we speculate that, in the layer formed with 7 watt power, the formation of a layer from largely intact silane also resulted in a network that bonded and constrained the amine groups within the interior of the layer. Fragmentation of the silane could produce ethoxy and alkyl amino radicals. One hypothesis is that insertion of alkyl amino radicals into the network at the surface of the growing film was responsible for creating the higher amount of surface reactive amines present in the film formed with a higher power.

The applicability of such coatings for biosensor platforms was demonstrated through an antibody/antigen bioassay, **Figure 5**. The APTES functionalized slides were employed in a typical sandwich immunoassay format using  $\alpha$ IgG and Cy5-labeled  $\alpha$ IgG as capture and detection antibodies respectively, and IgG as the model analyte. The limit-of-detection (corresponding to the background signal plus 3 times the

standard deviation of the background signal) was determined to be  $5.7 \text{ pg ml}^{-1}$  (**Figure 5**). This value is two orders of magnitude better than the ones obtained with immunosensors modified by silanization in solution (Boozer 2003, 2004, 2006; Raj 2009; Vikholm-Lundin and Albers 2006).

## 4. Conclusions

Cycloolefin polymer surfaces were successfully functionalized through the PECVD deposition of a new precursor, APTES, yielding amine functional groups available for biomolecule attachment. The deposition conditions were optimized in order to gain the most performant surface in attaching nanoparticles and DNA molecules. We identified the effect of plasma power in both activating and fragmenting the silane, and in both building the layer and eroding it. The consequences were that, in our system, whilst the thickness of the layer could be increased by increasing power and deposition time, the chemical functionality was optimal at a specific combination of parameters. We speculated that the effect of fragmentation of the silane into siloxane, ethoxy and alkyl amine radicals was the determining factor. An immunoassay performed using human IgG as a model analyte shows an improvement of the detection limit by two orders of magnitude beyond that obtained using devices activated by liquid-phase reaction. As the PECVD process is suitable for bulk processing and is environmentally friendly as it does not leave the liquid wastes, the amine functionalization of COP platforms using the methodology mentioned in this paper could potentially be used for bulk industrial processing of biosensors devices.

## **5. Acknowledgements:**

This material is based upon works supported by the Science Foundation Ireland (S.F.I.) under Grant No. 05/CE3/B754. D.E.W. is an E.T.S. Walton Visiting Fellow of Science Foundation Ireland. C.V. is a postdoctoral researcher of the Belgian Fund for Scientific Research (F.R.S./F.N.R.S.).

## 6. References

- Arriagada, F.J., Osseo-Asare, K., 1999. Synthesis of nanosize silica in a nonionic water-in-oil microemulsion: Effects of the water/surfactant molar ratio and ammonia concentration. *J. Colloids Interface Sci.* 211, 210-220.
- Arroyo-Hernández, M., Pérez-Rigueiro, J., Martínez-Duart, J.M., 2006. Formation of amine functionalized films by chemical vapour deposition. *Mater. Sci. Eng. C-Biomimetic Supramol. Syst.* 26, 938-941.
- Bae, I.-S., Jung, C.K., Cho, S.-J., Song, Y.-H., Boo, J.H., 2007. Characterization of organic polymer thin films deposited using the PECVD method. *J. Korean Phys. Soc.* 50, 1854-1857.
- Boozer, C., Yu, Q., Chen, S., Lee, C.Y., Homola, J., Yee, S.S., Jiang, S., 2003. Surface Functionalization for self-reflecting surface plasmon resonance (SPR) biosensors by multi-step self-assembly. *Sens. Actuators B.* 90, 22-30.
- Boozer, C., Ladd, J., Chen, S., Yu, Q., Homola, J., Jiang, S., 2004. DNA-directed protein immobilization on mixed ssDNA/oligo(ethylene glycol) self-assembled monolayers for sensitive biosensors. *Anal. Chem.* 76, 6967- 6972.
- Boozer, C., Ladd, J., Chen, S., Jiang, S., 2006. DNA-directed protein immobilization for simultaneous detection of multiple analytes by surface plasmon resonance biosensor. *Anal. Chem.* 78, 1515-1519.
- Cho, Y., Ivanisevic, A., 2004. SiO<sub>x</sub> surfaces with lithographic features composed of a TAT peptide. *J. Phys. Chem. B* 108, 15223-15228.
- Choi, I., Kim, Y., Kang, S.K., Lee, J. Yi, J., 2006. Phase separation of a mixed self-assembled monolayer prepared via a stepwise method. *Langmuir* 22, 4885-4889.
- Diaz-Quijada, G.A., Peytavi, R., Nantel, A., Roy, E., Bergeron, M.G., Dumoulin, M.M., Veres, T., 2007. Surface modification of thermoplastics – towards the plastic biochip for high throughput screening devices. *Lab Chip* 7, 856-862.
- Di Mundo, R., Ricci, M., d'Agostino, R., Fracassi, F., Palumbo, F., 2007. PECVD of low carbon content silicon nitride-like thin films with dimethylaminosilanes. *Plasma Process Polym.* 4, S21-S26.
- Dudek, M.M., Gandhiraman, R.P., Volcke, C., Cafolla, A.A., Daniels, S., Killard, A.J., 2009. Plasma surface modification of Cyclo-olefin polymers and its application to lateral flow bioassays. *Langmuir* 25, 11155-11161.
- Dudek, M.M., Gandhiraman, R.P., Volcke, C., Daniels, S., Killard, A.J., 2009. Evaluation of a range of surface modifications for the enhancement of lateral flow assays on Cyclic polyolefin micropillar devices. *Plasma Process Polym.* 2009, in press. DOI:10.1002/ppap.200900053.
- Dreesen, L., Silien, C., Volcke, C., Sartenaer, Y., Thiry, P.A., Peremans, A., Grugier, J., Marchand-Brynaert, J., Brans, A., Grubisic, S., Joris, B., 2007. Adsorption properties of the penicillin derivative DTPA on gold substrates. *ChemPhysChem* 8, 1071-1076.
- Finke, B., Schröder, K., Ohl, A., 2009. Structure retention and water stability of microwave plasma polymerized films from allylamine and acrylic acid. *Plasma Process Polym.* in press. DOI: 10.1002/ppap.200930305.
- Haïdopoulos, M., Mirabella, F., Horgnies, M., Volcke, C., Thiry, P.A., Rouxhet, P., Pireaux, J.J., 2007. Morphology of polystyrene films deposited by RF plasma. *J. Microscopy* 228, 227-239.
- Favia, P., Creatore, M., Palumbo, F., Colaprico, V., d'Agostino, R., 2001. Process control for plasma processing of polymers. *Surf. Coat. Technol.* 142-144, 1-6.

- Foose, L.L., Blanch, H.W., Radke, C.J., 2007. Immobilized protein films for assessing surface proteolysis kinetics. *J. Biotechnol.* 2, 32-37.
- Gandhiraman, R.P., Daniels, S., Cameron, D.C., 2007. A comparative study of characteristics of SiO<sub>x</sub>CyHz, TiO<sub>x</sub> and SiO-TiO oxide-based biocompatible coatings. *Plasma Process Polym.* 4, S369-S373.
- Gandhiraman, R.P., Karkari, S.K., Daniels, S., MacCraith, B.D., 2009. Influence of ion bombardment on the surface functionalization of plasma deposited coatings. *Surf. Coat. Tech.* 203, 3521-3526.
- Gomathi, N., Sureshkumar, A., Neogi, S., 2008. *Current Science* 94, 1478-1486.
- Gu, Q., Cheng, X., 2008. Tribological behaviors of self-assembled 3-aminopropyltriethoxysilane films on silicon. *Curr. Appl. Phys.* 8, 583-588.
- Jönsson, C., Aronsson, M., Rundström, G., Pettersson, C., Mendel-Hartvig, B., Bakker, J., Martinsson, E., Liedberg, B., MacCraith, B.D., Öhman, O., Melin, J., 2008. Silane-dextran chemistry on lateral flow polymer chips for immunoassays. *Lab chip* 8, 1191-1197.
- Jung, D., Yeo, S., Kim, J., Kim, B., Jin, B., Ryu, D.-Y., 2006. Formation of amine groups by plasma enhanced chemical vapour deposition and its application to DNA array. *Surf. Coat. Technol.* 200, 2886-2891.
- Kanan, S.M., Tze, W.T.Y., Tripp, C.P., 2002. Method to double the surface concentration and control the orientation of adsorbed (3-aminopropyl)dimethylethoxysilane on silica powders and glass slides. *Langmuir* 18, 6623-6627.
- Kameoka, J., Craighead, H.G., Zhang, H., Henion, J., 2001. A polymeric microfluidic chip for CE/MS determination of small molecules. *Anal. Chem.* 73, 1935-1941.
- Kim, J., Park, H., Jung, D., Kim, S., 2003. Protein immobilization on plasma-polymerized ethylenediamine-coated glass slides. *Anal. Biochem.* 313, 41-45.
- Kulisch, W., Lippmann, T., Kassing, R., 1989. Plasma-enhanced chemical vapour deposition of silicon dioxide using tetraethoxysilane as silicon source. *Thin Solid Films* 174, 57-61.
- Kurth, D.G., Bein, T., 1995. Thin films of (3-aminopropyl)triethoxysilane on aluminum oxide and gold substrates. *Langmuir* 11, 3061-3067.
- Kwon, Y., Coleman, M.A., Camarero, J.A., 2006. Selective immobilization of proteins onto solid supports through split-intein-mediated protein trans-splicing. *Angew. Chem. Int. Ed.* 45, 1726-1729.
- LaGraff, J.R., Chu-LaGraff, Q., 2006. Scanning force microscopy and fluorescence microscopy of microcontact printed antibodies and antibody fragments. *Langmuir* 22, 4685-4693.
- Laib, S., MacCraith, B.D., 2007. Immobilization of biomolecules on cycloolefin polymer supports. *Anal. Chem.* 79, 6264-6270.
- Mateo-Martí, E., Briones, C., Román, E., Briand, E., Pradier, C.M., Martín-Gago, J.A., 2005. Self-assembled monolayers of peptide nucleic acids on gold surfaces : A spectroscopic study. *Langmuir* 21, 9510-9517.
- Moon, J.H., Kim, J.H., Kang, T.-H., Kim, B., Kim, C.-H., Hahn, J.H., Park, J.W., 1997. Absolute surface density of amine group of the aminosilylated thin layers: ultraviolet-visible spectroscopy, second harmonic generation, and synchrotron-radiation photoelectron spectroscopy study. *Langmuir* 13, 4305-4310.
- Muguruma, H., Kase, Y., 2006. Structure and biosensor characteristics of complex between oxidase and plasma-polymerized nanothin film. *Biosens. Bioelectron.* 22, 737-743.

- Oh, S.J., Cho, S.J., Kim, C.O., Park, J.W., 2002. Characteristics of DNA microarrays fabricated on various aminosilane layers. *Langmuir* 18, 1764-1769.
- Qian, W., Yao, D., Xu, B., Yu, F., Lu, Z., Knoll, W., 1999. Atomic force microscopy studies of site-directed immobilization of antibodies using their carbohydrate residues. *Chem. Mater.* 11, 1399-1401.
- Raj, J., Herzog, G., Manning, M., Volcke, C., McCraith, B.D., Ballantyne, S., Thompson, M., Arrigan, D.W.M., 2009. Development of an antibody immobilisation method for sandwich immunoassay on cyclic olefin copolymer surfaces. *Biosen & Bioelectron.* 24, 2654-2658.
- Salmain, M., Fischer-Durand, N., Roche, C., Pradier, C.M., 2006. Immobilization of atrazine on gold, a first step towards the elaboration of an indirect immunosensor: characterization by XPS and PM-IRRAS. *Surf. Interface Anal.* 38, 1276-1284.
- Sethuraman, A., Han, M., Kane, R.S., Belfort, G., 2004. Effect of surface wettability on the adhesion of proteins. *Langmuir* 20, 7779-7788.
- Simon, A., Cohen-Bouhacina, T., Porté, M.C., Aimé, J.P., Baquey, C., 2002. Study of two grafting methods for obtaining a 3-aminopropyltriethoxysilane monolayer on silica surface. *J. Colloid Interface Sci.* 251, 278-283.
- Slocik, J.M., Beckel, E.R., Jiang, H., Enlow, J.O., Zabinski J.S., Bunning, T.J., Naik, R.R., 2006. Site-specific patterning of biomolecules and quantum dots on functionalized surfaces generated by plasma-enhanced chemical vapor deposition. *Adv. Mater.* 18, 2095-2100.
- Socrates, G., 2004. *Infrared and Raman Characteristic Group Frequencies*, Wiley VCH, Chichester.
- Song, S., Zhou, J., Qu, M., Yang, S., Zhang, J., 2008. Preparation and tribological behaviors of an amide-containing stratified self-assembled monolayers on silicon surface. *Langmuir* 24, 105-109.
- Sridharan, A., Muthuswamy, J., LaBelle, J.T., Pizziconi, V.B., 2008. Immobilization of functional light antenna structures derived from the filamentous green bacterium *Chloroflexus aurantiacus*. *Langmuir* 24, 8078-8089.
- Truica-Marasescu, F., Wertheimer, M.R., 2008. Nitrogen-rich plasma-polymer films for biomedical applications. *Plasma Process Polym.* 5, 44-57.
- Vikholm-Lundin, I., Albers, W., 2006. Site-directed immobilisation of antibody fragments for detection of C-reactive protein. *Biosen. & Bioelectron.* 21, 1141-1148.
- Wavhal, D.S., Zhang, J., Steen, M.L., Fisher, E.R., 2006. Investigation of gas phase species and deposition of SiO<sub>2</sub> films from HMDSO/O<sub>2</sub> plasmas. *Plasma Process Polym.* 3, 276-287.
- White, L.D., Tripp, C.P., 2000. Reaction of (3-aminopropyl)dimethoxysilane with amine catalysts on silica surfaces. *J. Colloid Interface Sci.* 232, 400-407.
- Zajíčková, L., Janča, J., Peřina, V., 1999. Characterization of silicon oxide thin films deposited by plasma enhanced chemical vapour deposition from octamethylcyclotetrasiloxane/oxygen feeds. *Thin Solid Films* 338, 49-59.
- Zhang, F., Srinivasan, M.P., 2004. Self-assembled molecular films of aminosilanes and their immobilization capacities. *Langmuir* 20, 2309-2314.

## 7. Figures

**Figure 1:** PMIRRAS spectra of bare cycloolefin polymer (COP) surfaces (black) and COP surfaces coated using the PECVD deposition of APTES at fixed deposition time (4 min) and varying RF plasma power of 7 watt (red), 14 watt (green) and 25 watt (blue). Three region of interest are highlighted: 1300-1000  $\text{cm}^{-1}$  (region 1), 1800-1500  $\text{cm}^{-1}$  (region 2) and 3500-3200  $\text{cm}^{-1}$  (region 3).

**Figure 2:** PMIRRAS spectra of bare cycloolefin polymer (COP) surfaces (black) and COP surfaces coated using the PECVD deposition of APTES at fixed RF plasma power (14 watts) and varying deposition time of 2 min (red), 4 min (green) and 8 min (blue). Three region of interest are highlighted: 1300-1000  $\text{cm}^{-1}$  (region 1), 1800-1500  $\text{cm}^{-1}$  (region 2) and 3500-3200  $\text{cm}^{-1}$  (region 3).

**Figure 3:** Graphical representation of the number of nanoparticles attached per micron square on different coated COP surfaces at fixed deposition time (left) and fixed RF plasma power (right).

**Figure 4:** Relative fluorescence unit measured after a fluorophore attachment (bottom) and DNA attachment (top) on the two preselected coatings, i.e. deposited at 7 watt and 14 watt both during 4 min deposition time.

**Figure 5.** Fluorescence linked immunosorbent assays for the detection of IgG as the model analyte. The measured limit-of-detection has improved by two orders of magnitude when compared with immunosensors that were prepared by silanization in solution.

**Table 1:** Table presenting (1) the thickness of the coating deposited through the PECVD process, as measured by ellipsometry; (2) the water contact angle and (3) the mean roughness of the coating surface (deduced from AFM imaging).

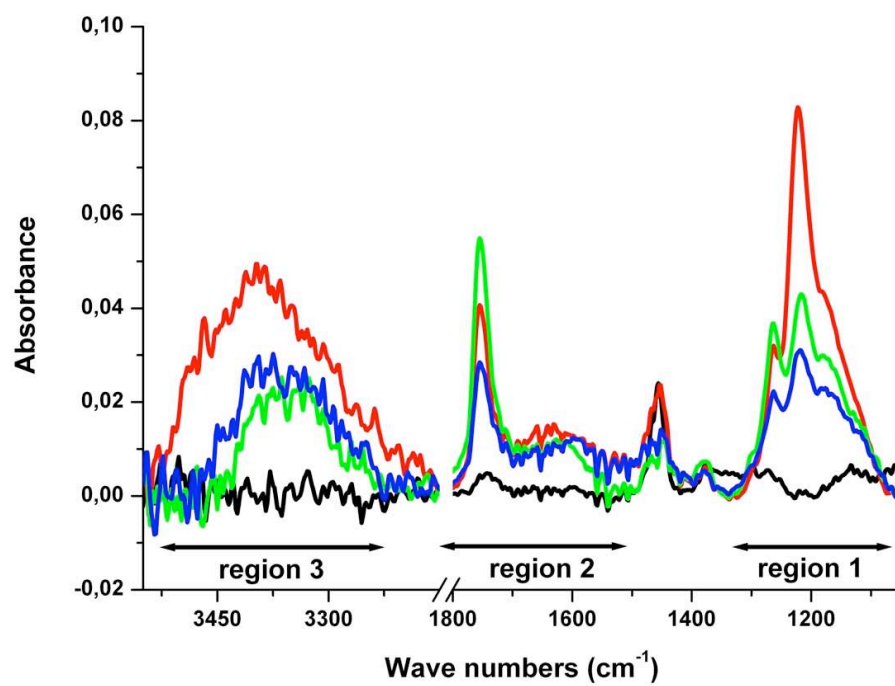


**Figure 1**

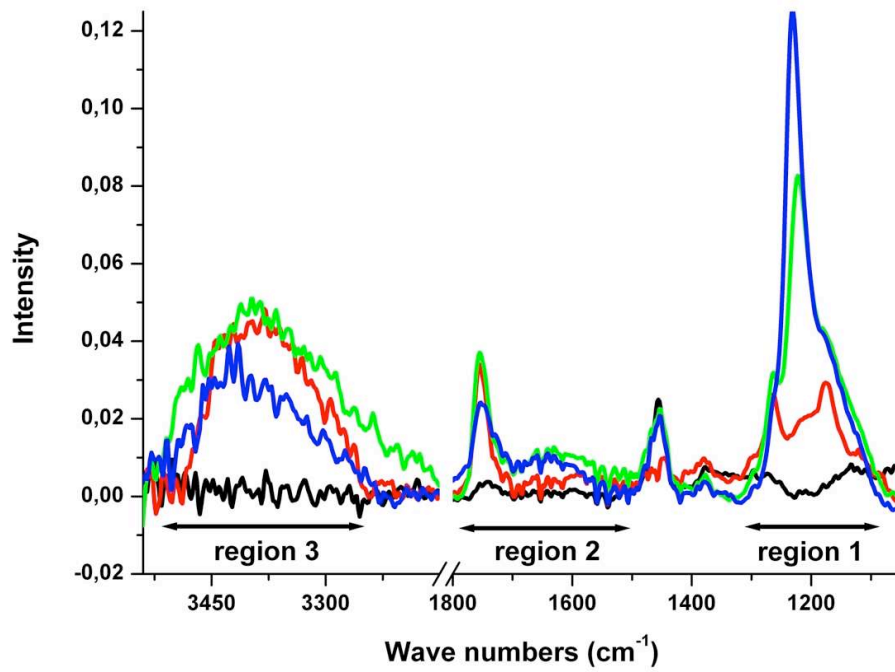
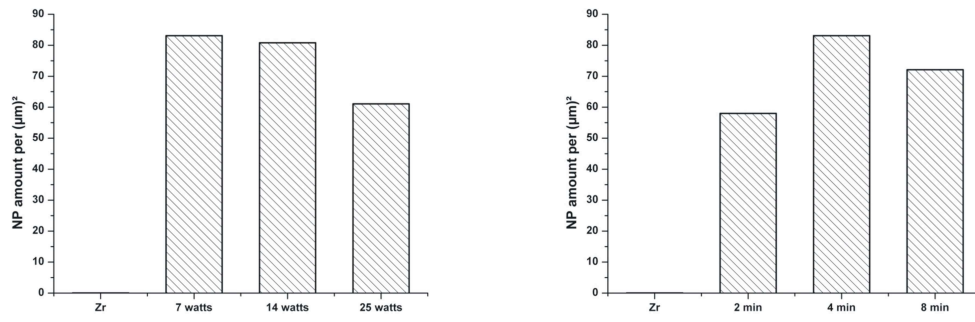
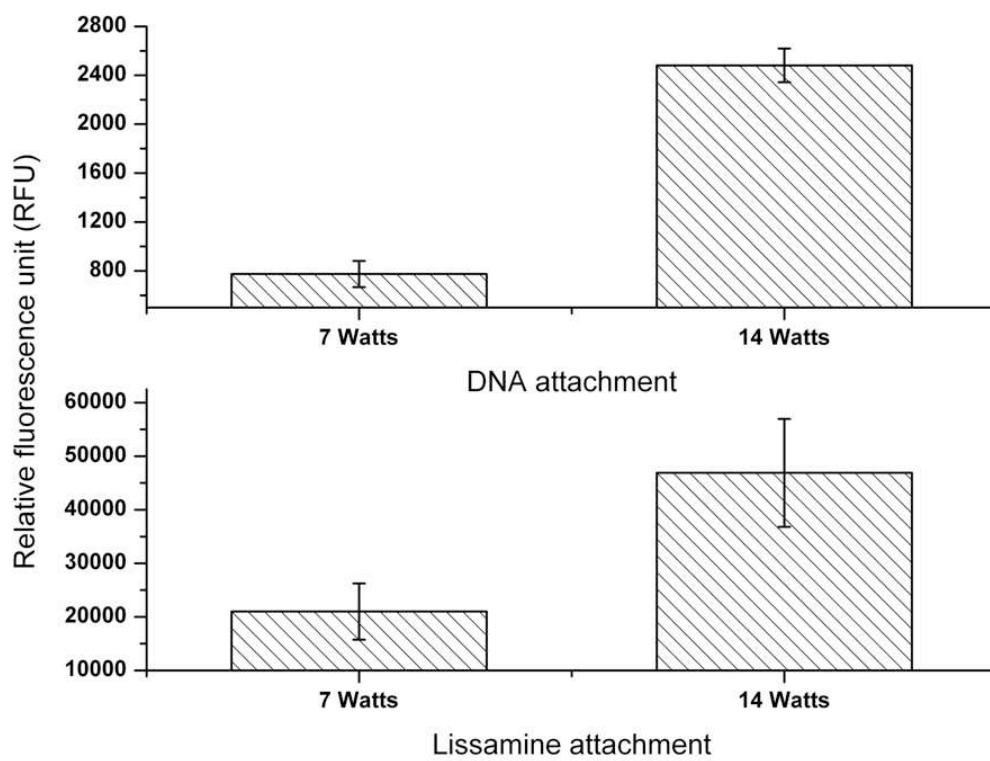


Figure 2



**Figure 3**



**Figure 4**

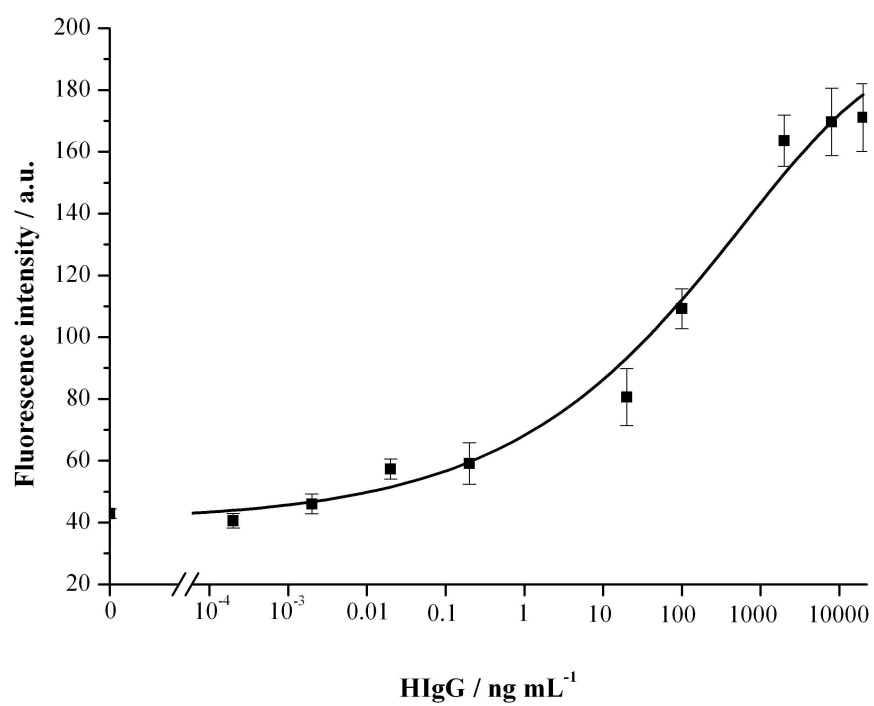


**Figure 5**

<b>Deposition conditions</b>	<b>Layer thickness (nm)</b>	<b>Water contact angle (°)</b>	<b>Surface roughness <math>R_{rms}</math> (nm)</b>
<b>4 min 7 watts</b>	<b>9.0 <math>\pm 0.1</math></b>	<b>58.2 <math>\pm 1.4</math></b>	<b>1.4 <math>\pm 0.3</math></b>
<b>4 min 14 watts</b>	<b>13.4 <math>\pm 0.3</math></b>	<b>60.6 <math>\pm 2.5</math></b>	<b>0.7 <math>\pm 0.1</math></b>
<b>4 min 25 watts</b>	<b><math>19.2 \pm 0.3</math></b>	<b><math>56.5 \pm 1.1</math></b>	<b>1.2 <math>\pm 0.2</math></b>
<b>14 watts 2 min</b>	<b><math>3.4 \pm 0.1</math></b>	<b><math>55.4 \pm 1.7</math></b>	<b><math>1.3 \pm 0.1</math></b>
<b>14 watts 4 min</b>	<b><math>13.4 \pm 0.3</math></b>	<b><math>58.2 \pm 1.4</math></b>	<b><math>0.7 \pm 0.1</math></b>
<b>14 watts 8 min</b>	<b><math>17.2 \pm 0.3</math></b>	<b><math>60.0 \pm 1.0</math></b>	<b><math>0.9 \pm 0.1</math></b>

**Table 1**